

## **A Comparison Study between Using SMES Unit and D-STATCOM in Improving Performance of FCWECS during Voltage Dip**

**A. M. Shiddiq Yunus<sup>1,a</sup>, Sonong Wahyudi<sup>1,b</sup>, Sukma Abadi<sup>1,c</sup>**

<sup>1</sup>*Energy Conversion Study Program, Mechanical Engineering Department,  
State Polytechnic of Ujung Pandang, Jl. Perintis Kemerdekaan KM. 10  
Makassar, 90245 Indonesia*

<sup>a</sup>*shiddiq@poliupg.ac.id*, <sup>b</sup>*sonongwahyudi@yahoo.com*, <sup>c</sup>*sukabadi2000@yahoo.com*

### **Abstract**

The penetration of wind turbine into the existing grid is increased during the past decades. The direct-drive variable speed, Full Converter Wind Energy Conversion System (FCWECS) was taking about 3500 Units of the whole installed wind turbines in 2014. In this paper, Superconducting Magnetic Energy Storage (SMES) Unit based on Hysteresis Current Control and Fuzzy Logic Control is applied to improve the performance of the system with FCWECS and compared to the system with generic model of D-STATCOM. The simulation was carried out using MATLAB/SIMULINK to verify the model under study. From the simulation results, it is obviously described that the performance of the system with FCWECS is much more improved with SMES Unit compared with the system with D-STATCOM.

**Keywords**— D-STATCOM, Fuzzy logic, SMES, Voltage Dip, and Wind Turbine.

### **1. Introduction**

The utilization of renewable energies nowadays is becoming more attractive due to the detrimental effects of the conventional energy sources to environment. The implementation of carbon tax in some countries has also been considered as a trigger to accelerate the utilization of renewable energies in some industrial countries. One of the most popular cleanness- renewable energy sources is wind energy. It is growth very amazingly from just less than 94,000 MW at the end of 2007 to 365,553 MW by the end of 2014 [1]. The future prospects of the global wind industry are very encouraging and it is estimated to grow by more than 70% over the next two years to

reach 160 GW by year 2012 and probable that by 2020 wind power will supply at least 10% of global electricity needs [2]. Since the improvement of power electronics technology, the number of wind turbine equipped with converter that injected into the network is increased. One of the variable-speed wind turbines is type-D or classified as full converter wind energy conversion system (FCWECS). A low speed multipole synchronous ring generator with the same rotational speed as the wind turbine rotor converts the mechanical energy into electricity. The generator can have a wound rotor or a rotor with permanent magnets. The stator is not coupled directly to the grid but to a power converter or a diode rectifier with a single voltage source converter (VSC). The electronic converter makes it possible to operate the wind turbine at variable speed. The trend shows that FCWECS is increased in the market share and reach about 3500 Units in 2014 [3]. The typical configuration of FCWECS is shown in Fig. 1.

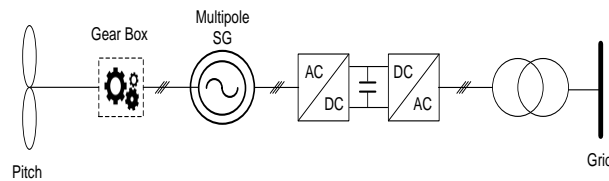


**Figure 1. Typical of FCWECS**

As aforementioned that about 3500 Units of FCWECS is installed world widely. This existing WTGs however, might be were not designed to comply the recent requirements of grid code that wind turbine generators (WTGs) have to be able to withstand in certain level of fault to assure the continuity of supplying power to the grid (where in the earlier stages of integrating WTG into the grid, WTGs are allowed to be disconnected from the grid to avoid damages during the fault at the grid side), therefore one common strategy to fulfill this requirement is by connecting FACTS devices which be able to prevent the WTGs from being disconnected from the grid [4]. Since the successful of installing 30 MJ of SMES Unit at Bonneville Power Company in 1982 [5], superconducting magnetic has attractive the researchers to study intensively for various application in power system as described in [6]. Superconducting magnetic energy storage (SMES) systems store energy in the magnetic field created by the flow of direct current in a coil of cryogenically cooled, superconducting material.

An SMES system includes a superconductor coil, a power condition system, a cryogenic refrigerator, and a cryostat/vacuum vessel to keep the coil at a low temperature that is required to maintain the coil in superconducting state and thus, allow it to be highly efficient in storing electricity where the efficiency of SMES is in the range of 95-98% [7]-[11]. The other advantages of SMES Unit are including very quick response, possible for high power application and working in four-quadrant [12]. Another popular FACTS device that widely used in power system is STATCOM (Static Synchronous Compensator) where for middle voltage application sometime is

called distributed-STATCOM (D-STATCOM). In variable speed wind turbine generator application, most of D-STATCOM were studied is for WTGs that equipped with doubly fed induction generator (DFIG) as can be found in Refs [13]-[18]. In this paper, a comparison study is carried out between connecting the SMES Unit and D-STATCOM into the system that is integrated with FCWECS during fault in the grid side. A SMES configuration system used in this paper consists of hysteresis current control in conjunction with fuzzy logic control where had been introduced earlier in author works in Ref [19, 20]. D-STATCOM model used as comparator in this paper is the model that provided in Ref [15]. Simulink/Matlab software is used to simulate the model and verify the results.

## 2. System under Study

The system under study is depicted in Fig. 2. It consists of five-2 MW FCWECS connected through bus 25 KV. The FCWECS presented in this paper consists of a synchronous generator connected to a diode rectifier, a DC-DC IGBT-based PWM boost converter and a DC/AC IGBT-based PWM converter. The system is able to control reactive and active power quickly and then the turbine may take part in the power system control [21]. The control system of DC-DC converter is used to maintain the speed at 1 pu. The reactive power produced by the wind turbine is regulated at 0 MVar in normal condition where no reactive power is transferred to the grid in normal condition. For a wind speed of 15 m/s which is used in this study, the turbine output power is 1 pu and the generator speed is 1 pu [22]. SMES Unit is connected to the bus 25 KV and assumed that it has been fully charged at its maximum capacity of 1 MJ.

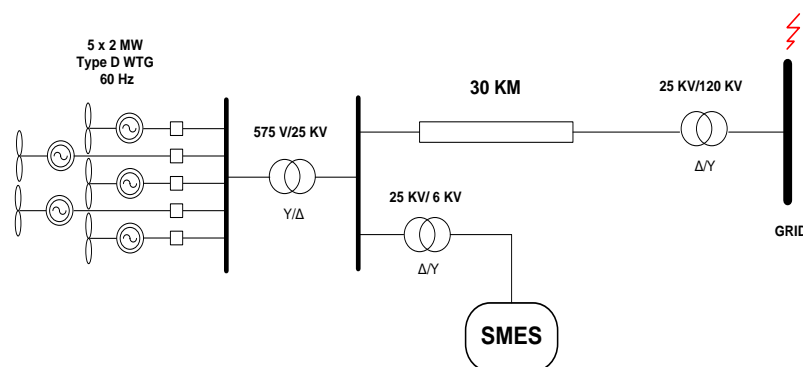


Figure 2. Systems under Study

## 3. SMES Unit Configuration and Control System

### 3.1. Hysteresis Current Control (HCC)

HCC is widely used because of its simplicity, ease to implement, insensitivity to load parameters variations, fast dynamic response and applicable for maximum current limit [23]. The basic implementation of hysteresis current control is based on deriving

the switching signals from the comparison of the current error with a fixed tolerance band. This control is based on the comparison of the actual phase current with the tolerance band around the reference current associated with that phase.

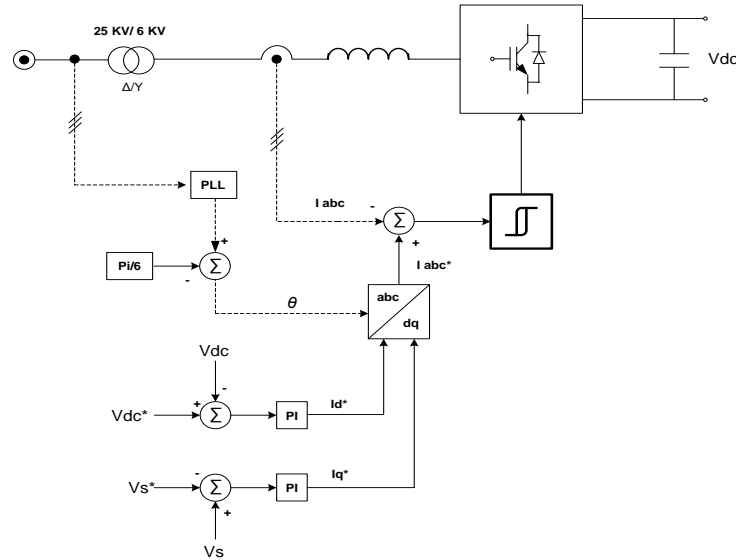


**Figure 3. Control algorithm of the SMES [19]**

On the other hand, this type of band control is negatively affected by the phase current not only depends on the corresponding phase voltage but is also affected by the voltage of the other two phases [24]. Natural phenomena occur regarding effect of interference between phases (referred as inter-phases dependency) which can lead to high switching frequency. To maintain the advantages of the hysteresis methods, this phase independency can be minimized by using phase-locked loop (PLL) technique to constrain the inverter switching at a fixed predetermined frequency [25]. HCC is comparing the 3-phase line currents ( $I_{abc}$ ) with the reference current ( $I_{abc}^*$ ) which is dictated by the  $I_d^*$  and  $I_q^*$  references. The value of  $I_d^*$  and  $I_q^*$  are generated through the conventional PIs controller both from error values of  $V_{dc}$  and  $V_s$ . The value of  $I_d^*$  and  $I_q^*$  is converted through the Park Transformation ( $dq0-abc$ ) method to produce reference current ( $I_{abc}^*$ ) as shown in Fig. 3. The proposed control algorithm in this paper is much simpler and closer to realistic application compared with controller in Ref [26], where 4 PIs controller were used meaning that more time consume to find the best optimal tune parameters of the PIs, moreover only  $P_g$  was used as input in the DC-DC Chopper and ignore the energy capacity of the SMES [27]. Typical hysteresis current input and switching signal from hysteresis current control can be seen in Fig. 4 (a) and (b) respectively.

### 3.2. Fuzzy Logic Controller (FLC)

To control the transfer power between SMES coil and the system, the DC-DC Chopper is used and Fuzzy logic is selected to control the duty cycle ( $D$ ) of the DC-

DC Chopper due to its advantages including cover much wider range of operating condition, suitable for uncertainty condition and no needs complex mathematical model, therefore easy to learn and modify the rules [28].

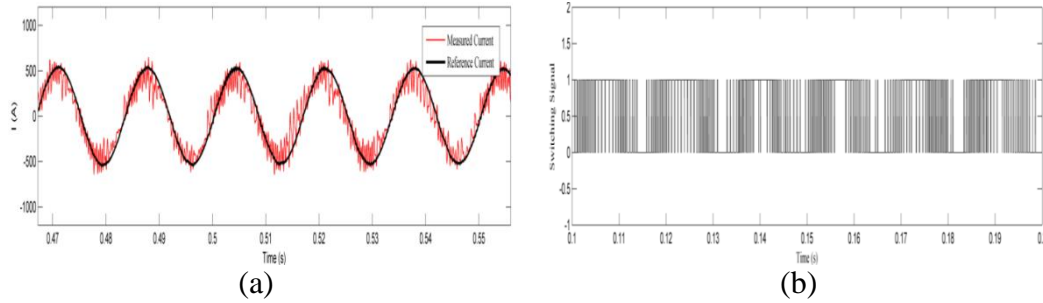


**Figure 4. (a) Typical Hysteresis Current and (b) Typical switching signal for VSC**

The stored energy in the SMES coil can be calculated as:

$$E = \frac{1}{2} I_{SM}^2 L_{SM} \tag{1}$$

Where  $E$  is the SMES energy in Joule;  $I_{sm}$  is the SMES Current (A) and  $L_{sm}$  is the SMES inductor coil.

The fuzzy logic controller (FLC) is developed according to the fuzzy inference flow which is a process of formulating the mapping from a given input to the designated output. Input variables for the model are the real power of FCWECS and SMES coil current. The output of FLC is duty cycle ( $D$ ) for generating signal for DC-DC Chopper as shown in Fig. 5. This duty cycle will determine whether the power is transferred to/absorbed from the power system or in standby condition (no coil action). The operation range of duty cycle can be seen in Table 1.

**Table 1. Rules of Duty Cycle**

| Duty Cycle (D)   | SMES Coil Action      |
|------------------|-----------------------|
| $D = 0.5$        | standby condition     |
| $0 \leq D < 0.5$ | discharging condition |
| $0.5 < D \leq 1$ | charging condition    |

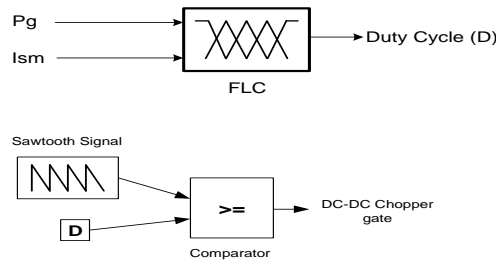


**Figure 5. Control algorithm of DC-DC Chopper [19]**

If duty cycle ( $D$ ) is equal to 0.5, no action will be taken by the coil, in this condition system is defined as a normal condition, when power in the system is reduced,  $D$ , depends on the reduced power, will be reduced accordingly within 0 to 0.5. Charging process of the coil will be in the range of 0.5 to 1.

The model is built using the graphical user interface tool provided by MATLAB. Each input was fuzzified into five sets of trimf type of membership function (MF). The triangular curve is a function of a vector,  $x$ , and depends on three scalar parameters  $a$ ,  $b$ , and  $c$  as given by:

$$f(a, b, c) = \max\left(\min\left(\frac{x-a}{b-a}, \frac{c-x}{c-b}\right), 0\right) \tag{2}$$

The parameters  $a$  and  $c$  locate the "feet" of the triangle and the parameter  $b$  locates the peak [29],[30]. The corresponding function curve for each input variables are shown in Fig. 7 (a) and (b).

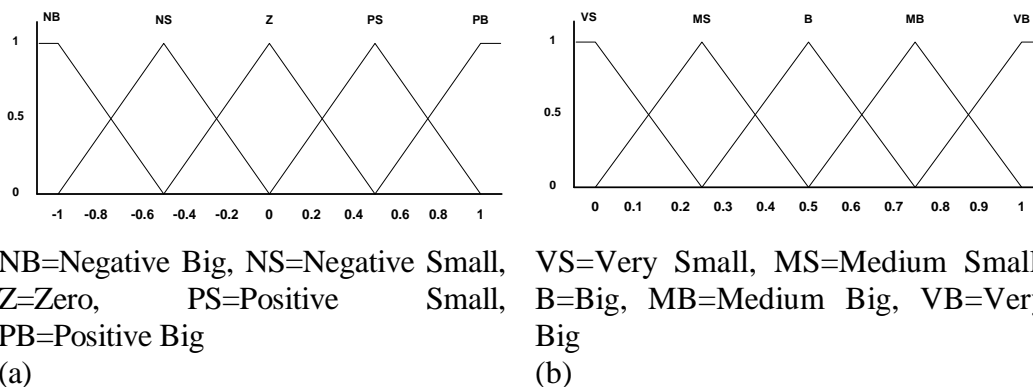
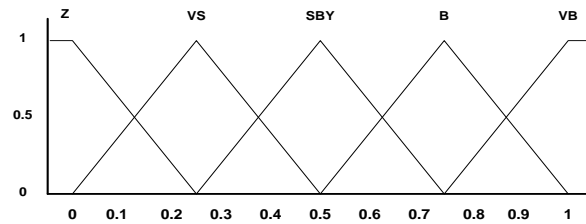


**Figure 7. Input Variable (a) MF –  $\Delta P$  (pu) and (b) Input Variable MF –  $\Delta I_{SMES}$  (pu)**

Result of fuzzification from each input was then applied with fuzzy operator in the antecedent and related to the consequence, by application method. The

membership functions for the output variables (duty cycle) are considered on the scale 0 to 1 as shown in Fig. 8.



Z=Zero, VS=Very Small, SBY=Stand-By, B=Big, VB=Very Big

**Figure 8. Output variable MF – Duty cycle**

**4. D-STATCOM Configuration**

D-STATCOM is one of the promising technologies applied to improve power system performance. The advantages of D-STATCOM include fast response time, better voltage support capability and reactive power support at low voltage levels. Moreover, it does not require thyristor-controlled reactors (TCR) or thyristor-switched capacitors (TCS) and does not produce low harmonic order distortions [31],[32]. D-STATCOM mainly consists of a pulse width modulation (PWM) voltage source converter (VSC) with a capacitor in the DC side, coupling transformer and control system as shown in Fig. 9. The interaction between the grid voltage and the voltage at the D-STATCOM ac side provides the control of reactive power flow. The control system enables adapted regulation of bus voltage and the DC voltage levels and hence controlling the reactive power flow according to the system requirements. The VSC consists of 12 pulse IGBT converter station to minimize the harmonics generated from switching operation.

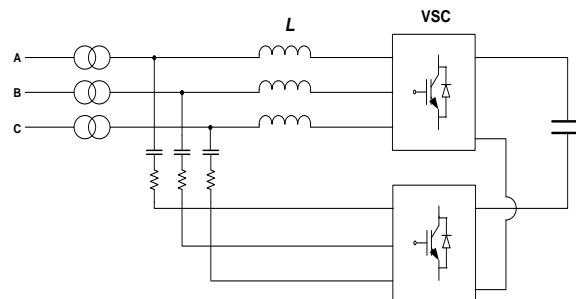


**Figure 9. D-STATCOM configuration**

The basic principle of D-STATCOM operation is illustrated in Fig. 10. If the voltage at the D-STATCOM terminals is higher than the grid voltage (Fig. 10 (a)), reactive power will be injected from D-STATCOM to the grid and D-STATCOM will

behave as a capacitor. When the voltage at the D-STATCOM is less than the grid voltage (Fig. 10 (b)), D-STATCOM will behave as an inductor and reactive power flow will be reversed. Under normal operating conditions, both voltages will be equal and there will be no power exchange between the D-STATCOM and the grid. The detailed control system of the D-STATCOM is shown in Fig. 11 [30]. In this system, the DC Voltage across the capacitor, the grid three-phase currents and three-phase voltages at the PCC are sensed and converted to the  $d-q$  reference frame to create  $I_d$ ,  $I_q$ ,  $V_d$  and  $V_q$ . These parameters in  $d-q$  reference frame are then compared with the corresponding nominal values to create error signals ( $\Delta I_d$ ,  $\Delta I_q$  and  $\Delta V_{AC}$ ) which are fed to PID/PI controller to create Modulation Index (MI) and phase angle (Phi) required for the voltage source converter (VSC) switching operation.

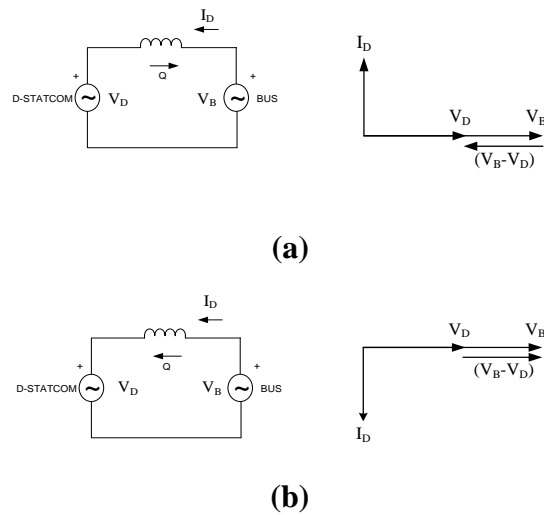


Figure 10. D-STATCOM principle of operation

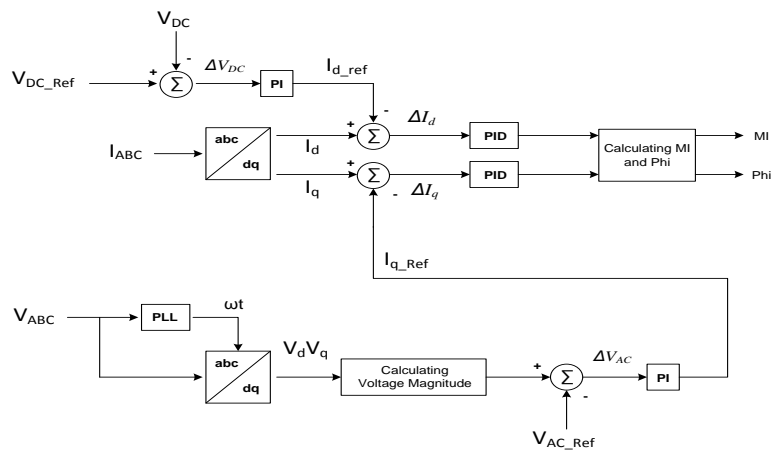
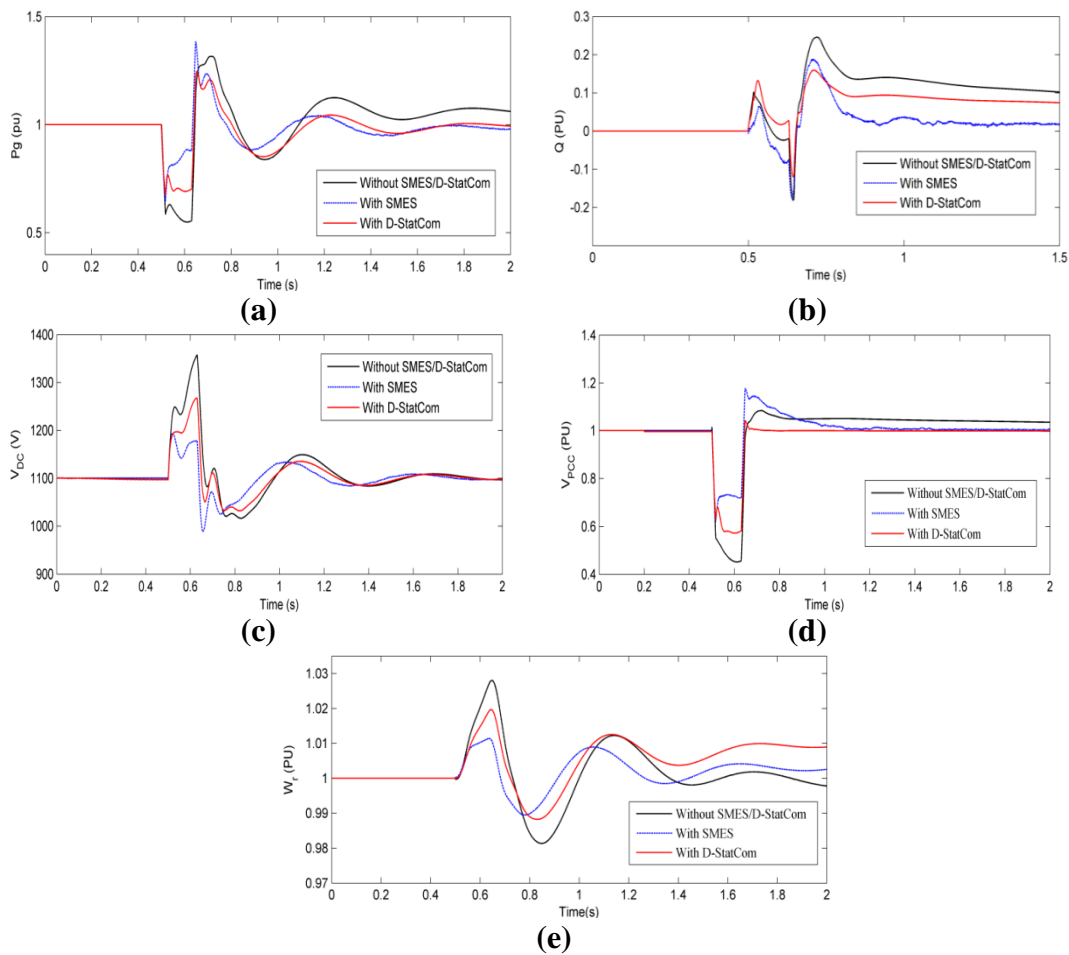


Figure 11. Control system of D-STATCOM



**5. Simulation Results and Discussion**

In this study, a voltage dip depth of 0.5 pu is applied lasting for 0.13s before the fault is cleared in the grid side. Both SMES Unit and D-STATCOM will be applied to investigate the dynamic behavior of the system during the fault. As can be seen in Fig 12 (a), during voltage dip, without any SMES or D-STATCOM, power produced from the WTG will fall until 0.55 pu, however, when D-STATCOM is connected only about 0.15 pu while when SMES is connected, power can be saved about 0.35 pu and the power will reach the steady state faster. This is also observable in Fig 12 (b), where reactive power produced by WTG will reach the steady state condition in 0.07 s (return to zero) after fault is cleared while the D-STATCOM can only support the WTGs slightly. DC voltage is another important parameter in WTG equipped with converters. In some manufactures, high overshoot of DC voltage can lead to the relay to stop the converter to switching.



**Figure 12. FCWECS Responses during Voltage Dip**

Fig 12 (c) shows that by connecting SMES Unit, the overshoot of DC voltage can be reduced to 1.1 pu while with and without D-STATCOM the overshoot of DC voltage can reach about 1.14 pu and 1.23 pu respectively. The significant of connecting SMES unit is also shown in Fig. 12 (d), where the voltage drop at the PCC (point of common coupling) can be reduced about 0.3 pu while with D-STATCOM it will reduced only about 0.15 pu. It is naturally that during the fault, the rotor speed of SG will oscillate and may lead to instability in the overall system, however with SMES connected, this oscillation can be suppressed, decrease the maximum overshooting and decrease the settling time as can be confirmed from the generator shaft speed shown in Fig. 12 (e). The figure also shown that D-STATCOM can only give small contribution in reducing the overshoot, moreover the settling time is still large and might not be able to avoid the instability of the system.

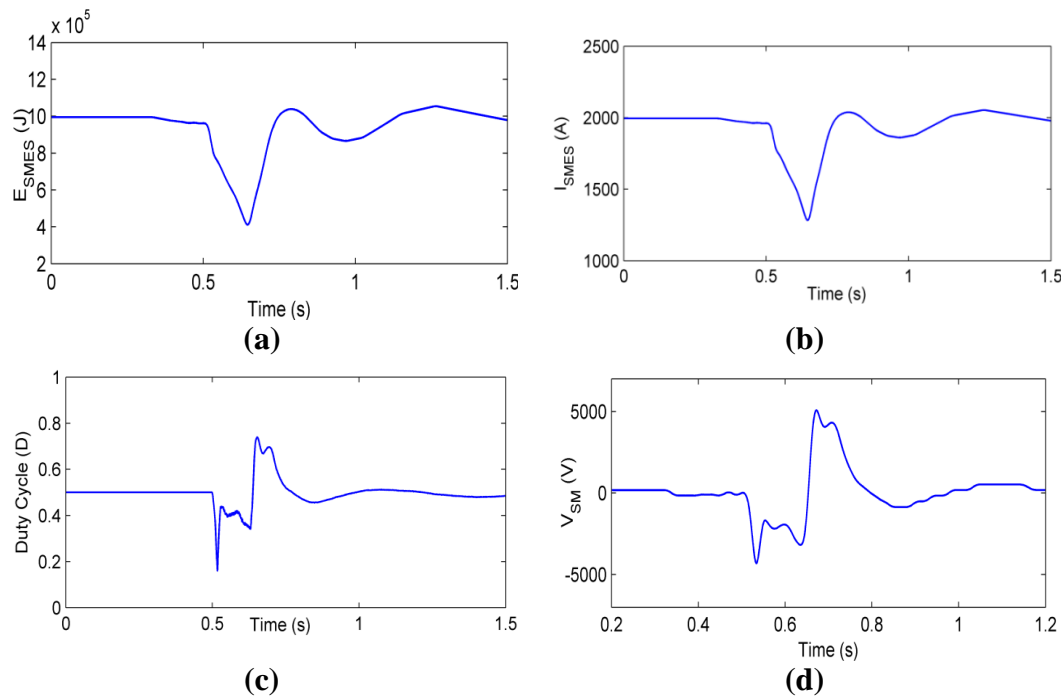


**Figure 13. SMES Unit Responses during Voltage Dip**

Fig. 13 (a)-13 (d) depicts the SMES Unit behavior during the voltage dip. The behavior of SMES coil current is the same with the SMES unit energy produced since the current is the direct function of the energy produced by the coil as stated in equation (1). Duty cycle behavior is shown in Fig 13 (c). Before voltage dip occurs in the grid side, SMES Unit control detects no different between the reference-power with the measured one ( $\Delta P=0$ ) and the SMES coil current has reached its maximum value, therefore, the value of the duty cycle ( $D$ ) is remained constant at 0.5. When voltage dip occurs at 0.5 s, the controller will evaluate the different power ( $\Delta P$ ) and the SMES coil current value ( $I_{SM}$ ) to decide the value of duty cycle. When real power is drop, SMES unit will soon

provide power and in this condition duty cycle will be in the range of  $0 \leq D < 0.5$  and will be in the range of  $0.5 < D \leq 1$  as in charging position when the condition is return to normal (fault is cleared). Once the peak value of SMES coil current is reached,  $D$  will return to 0.5. Fig. 13 (d) describes the value  $V_{SM}$ , where the value goes to negative in discharging position and goes to positive in charging position, again, the  $V_{SM}$  value will return to zero when no transfer power to/from the main system.

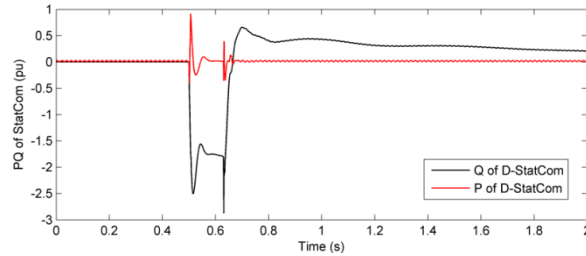


**Figure 14. D-STATCOM Responses during Voltage Dip**

The active and reactive power of D-STATCOM is depicted in Fig. 14. As can be noticed that it is very limited active power can be contributed from D-STATCOM to the system, however, transfer and absorbing reactive power from D-STATCOM is giving more contribution to the system during the fault.

**6. Conclusion**

The proposed control algorithm of SMES Unit that consists of Hysteresis Current Controller and Fuzzy Logic Controller is presented. From the simulation results it obviously can be investigated that the SMES unit configuration is very effective in improving the performance of the power system with FCWECS during voltage dip at the grid side compared with the D-STATCOM. The proposed control algorithm of the SMES unit is simple and easy to implement and able to improve the fault ride through of the WTG. The SMES Unit, in the other hand is still costly equipments, however due to the invention of superconducting material which is able to operate in high temperature, the SMES unit will no longer is economically viable in market niece.

**Appendices**

**Table 2. Parameters of Simulated D-STATCOM**

|                      |        |
|----------------------|--------|
| Rated Reactive Power | 3 MVAr |
|----------------------|--------|

**Table 3. Parameters of Simulated FCWECS**

|                |                    |
|----------------|--------------------|
| Rated Power    | 10 MW (5 x @ 2 MW) |
| Stator Voltage | 575 V              |
| Frequency      | 60 Hz              |
| $R_S$          | 0.006 pu           |
| $V_{DC}$       | 1100 V             |

**Table 4. Parameters of Simulated SMES Unit**

|                |        |
|----------------|--------|
| Rated Energy   | 1 MJ   |
| $L_{SM}$       | 0.5 H  |
| Rated $I_{SM}$ | 2000 A |

**Reference**

- [1] www.gwec.net, 22 February 2015.
- [2] P. Musgrove, *Wind Power*, New York: Cambridge University Press, 2010, pp. 221-222.
- [3] www.plantengineering.com, accessed, 22 February 2015.
- [4] J. G. Slootweg, S. W. H. de Haan, H. Polinder, and W. L. Kling, "General model for representing variable speed wind turbines in power system dynamics simulations", *IEEE Transactions on, Power Systems*, vol. 18, pp. 144-151. 2003
- [5] H. J. Boenig and J. F. Hauer, "Commissioning Tests Of The Bonneville Power Administration 30 MJ Superconducting Magnetic Energy Storage Unit", *IEEE Transactions on Power Apparatus and Systems*, , vol. PAS-104, pp. 302-312.1985
- [6] M. H. Ali, W. Bin, and R. A. Dougal, "An Overview of SMES Applications in Power and Energy Systems", *IEEE Transactions on Sustainable Energy*, vol. 1, pp. 38-47. 2010
- [7] P. F. Ribeiro, B. K. Johnson, M. L. Crow, A. Arsoy, and Y. Liu, "Energy storage systems for advanced power applications", *Proceedings of the IEEE*, vol. 89, pp. 1744-1756. 2001
- [8] S. M. Schoenung. "Characteristics and Technologies for Long- vs. Short-Term Energy Storage," <http://prod.sandia.gov/techlib/access-control.cgi/2001/010765.pdf>, accessed. 20 February, 2014
- [9] S. C. Smith, P. K. Sen, and B. Kroposki, "Advancement of energy storage devices and applications in electrical power system," in *Power and Energy Society General Meeting - Conversion and Delivery of Electrical Energy in the 21st Century, 2008 IEEE*, 2008, pp. 1-8.
- [10] H. Chen, T. N. Cong, W. Yang, C. Tan, Y. Li, and Y. Ding, "Progress in electrical energy storage system: A critical review", *Progress in Natural Science*, vol. 19, pp. 291-312. 2009

- [11] S. Faias, P. Santos, J. Sousa, and R. Castro. "An Overview on Short and Long-Term Response Energy Storage Devices for Power Systems Applications," <http://www.icrepq.com/icrepq-08/327-faias.pdf>, accessed. 20 February, 2014
- [12] E. Acha, V. G. Agelidis, O. Anaya-Lara, and T. J. E. Miller, *Power Electronic Control in Electrical System*, Oxford: Newnes, 2002, pp. 239.
- [13] S. Bozhko, R. Li, R. Blasco-Gimenez, G. M. Asher, J. C. Clare, L. Yao, and C. Sasse, "STATCOM-controlled HVDC Power Transmission for Large Offshore Wind Farms: Engineering Issues," in *IEEE Industrial Electronics, IECON 2006 - 32nd Annual Conference on*, 2006, pp. 4219-4224.
- [14] M. Fazli, A. R. Shafighi, A. Fazli, and H. A. Shayanfar, "Effects of STATCOM on wind turbines equipped with DFIGs during grid faults," in *World Non-Grid-Connected Wind Power and Energy Conference (WNWEC), 2010*, pp. 1-4
- [15] C. Liu, Y. Kang, J. Chen, L. Kevin, X. Lin, X. Liu, and F. Xu, "Simplified Active and Reactive Power Control of Doubly Fed Induction Generator and the Simulation with STATCOM," in *Applied Power Electronics Conference and Exposition, 2009. APEC 2009. Twenty-Fourth Annual IEEE*, 2009, pp. 1927-1931.
- [16] Q. Wei, G. K. Venayagamoorthy, and R. G. Harley, "Real-Time Implementation of a STATCOM on a Wind Farm Equipped With Doubly Fed Induction Generators", *IEEE Transactions on Industry Applications*, vol. 45, pp. 98-107.2009
- [17] M. Zengqiang, C. Yingjin, L. Liqing, and Y. Yang, "Dynamic performance improvement of wind farm with doubly fed induction generators using STATCOM," in *International Conference on Power System Technology (POWERCON), 2010*, pp. 1-6.
- [18] B. Pokharel and G. Wenzhong, "Mitigation of disturbances in DFIG-based wind farm connected to weak distribution system using STATCOM," in *North American Power Symposium (NAPS), 2010*, pp. 1-7.
- [19] A. M. Shiddiq-Yunus, M. A. S. Masoum, and A. Abu-Siada, "Application of SMES to Enhance the Dynamic Performance of DFIG During Voltage Sag and Swell", *IEEE Transactions on Applied Superconductivity*. vol. 22, Issue: 4, p. 5702009, Aug. 2012.
- [20] A. M. Shiddiq Yunus, A. Abu Siada, and M. A. S. Masoum "Application of SMES Unit to Improve DFIG Power Dispatch and Dynamic Performance During Intermittent Misfire and Fire-Through Faults", *Journal IEEE Transaction on Applied Superconductivity*. Vol. 23, No. 4 August 2013.
- [21] F. Blaabjerg and Z. Chen, *Power Electronics for Modern Wind Turbines*, Aalborg: Morgan & Claypool Publishers, 2006, pp. 18.
- [22] [http://www.mathworks.com/products/simpower/demos.html?file=/products/demos/shipping/powersys/power\\_wind\\_type\\_4\\_avg.html](http://www.mathworks.com/products/simpower/demos.html?file=/products/demos/shipping/powersys/power_wind_type_4_avg.html), accessed. 15 October 2014.
- [23] K. Bong-Hwan, K. Tae-Woo, and Y. Jang-Hyoun, "A novel SVM-based hysteresis current controller", *IEEE Transactions on Power Electronics*, vol. 13, pp. 297-307.1998

- [24] M. Milosevic. "Hysteresis Current Control in Three-Phase Voltage Source Inverter," [http://www.eeh.ee.ethz.ch/uploads/tx\\_ethpublications/milosevic\\_hysteresis.pdf](http://www.eeh.ee.ethz.ch/uploads/tx_ethpublications/milosevic_hysteresis.pdf), accessed. 19 February, 2014
- [25] L. Malesani and P. Tenti, "A novel hysteresis control method for current-controlled voltage-source PWM inverters with constant modulation frequency", *IEEE Transactions on Industry Applications*, vol. 26, pp. 88-92.1990
- [26] M. H. Ali, P. Minwon, Y. In-Keun, T. Murata, and J. Tamura, "Improvement of Wind-Generator Stability by Fuzzy-Logic-Controlled SMES", *IEEE Transactions on Industry Applications*, vol. 45, pp. 1045-1051.2009
- [27] A. M. Shiddiq-Yunus, A. Abu-Siada, and M. A. S. Masoum: 'Effects of SMES on Dynamic Behaviors of Type D-Wind Turbine Generator-Grid Connected during Short Circuit '. *IEEE PES General Meeting, Detroit, Michigan, USA*, 26-29 July 2011.
- [28] L. Reznik, *Fuzzy controllers*, Oxford; Boston: Newnes, 1997.
- [29] <http://www.mathworks.com/help/toolbox/fuzzy/trimf.html>, accessed. 15 October 2014,
- [30] H. Li and M. M. Gupta, *Fuzzy Logic and Intelligent System*, Massachusetts: Kluwer Academic Publisher, 1995, pp. 8
- [31] H. Chong, A. Q. Huang, M. E. Baran, S. Bhattacharya, W. Litzenberger, L. Anderson, A. L. Johnson, and A. A. Edris, "STATCOM Impact Study on the Integration of a Large Wind Farm into a Weak Loop Power System", *IEEE Transactions on Energy Conversion*, , vol. 23, pp. 226-233. 2008
- [32] P. Giroux, G. Sybille, and H. Le-Huy, "Modeling and simulation of a distribution STATCOM using Simulink's Power System Blockset," in *Industrial Electronics Society, 2001. IECON '01. The 27th Annual Conference of the IEEE*, pp. 990-994 vol.2. 2001.